



Manganese Catalysed Dehydrocoupling of Silanes and Siloxanes with Ammonia to Prepare Oligosilazanes and Polysiloxazanes

Journal:	<i>Dalton Transactions</i>
Manuscript ID	DT-ART-07-2024-001982
Article Type:	Paper
Date Submitted by the Author:	10-Jul-2024
Complete List of Authors:	Mehta, Gautam; Arizona State University, School of Molecular Sciences Nguyen, Thao; Arizona State University, School of Molecular Sciences Flores, Marco; Arizona State University, School of Molecular Sciences Trovitch, Ryan; Arizona State University, School of Molecular Sciences

Manganese Catalysed Dehydrocoupling of Silanes and Siloxanes with Ammonia to Prepare Oligosilazanes and Polysiloxazanes

Gautam K. Mehta, Thao T. Nguyen, Marco Flores and Ryan J. Trovitch*

Received 00th January 20xx,
Accepted 00th January 20xx

DOI: 10.1039/x0xx00000x

The halogen-free synthesis of oligosilazanes has been observed upon dehydrocoupling silanes with ammonia at 25 °C using $[(2,6\text{-iPr}_2\text{PhBDI})\text{Mn}(\mu\text{-H})_2]$. Extending this methodology to polymethylhydrosiloxanes afforded thermally robust polysiloxazane solids, and the dehydrocoupling of 1,3,5,7-tetramethylcyclotetrasiloxane with ammonia afforded a polysiloxazane having a weight-average molecular weight of 4300 g/mol. A representative oligosilazane has been applied to a copper surface and found to afford a 20 μm thick coating that resists corrosion after 24 h under water. Addition of ammonia to $[(2,6\text{-iPr}_2\text{PhBDI})\text{Mn}(\mu\text{-H})_2]$ allowed for characterization of the catalyst resting state, $[(2,6\text{-iPr}_2\text{PhBDI})\text{Mn}(\mu\text{-NH}_2)]_2$, which has been found to mediate Si–N dehydrocoupling.

Introduction

Polysilazanes, which feature a repeating Si–N backbone,¹ can be cured by moisture to afford corrosion-resistant coatings.² The most cost-effective polysilazane formulations are produced by adding NH_3 to a mixture of Me_2SiCl_2 and MeSiHCl_2 , which yields cyclic and linear silazanes (Fig. 1, a) along with one equivalent of $[\text{NH}_4][\text{Cl}]$ waste for each Si–N bond that is formed.³ It is often desirable to apply and cure polysilazanes at room temperature, which requires the addition of 3-triethoxy-1-propanamine as a crosslinking agent.⁴ The glass-like coatings that are obtained are indispensable in the transportation industry for extending the lifetime of metal surfaces.⁵

The dehydrocoupling of Si–H and N–H bonds is a promising alternative to chlorosilane ammonolysis that generates H_2 as a value-added by-product (Fig. 1, b).^{6–8} Well-defined catalysts that span the periodic table have been developed for Si–H and N–H dehydrocoupling; however, they have mainly been utilized for the silylation of primary or secondary amines.⁸ The coordination of NH_3 can inhibit dehydrocoupling,⁹ and the use of bulky

tertiary silanes has limited dehydrocoupling to monosilylamine formation.^{9,10} In a highly influential study, Laine and co-workers demonstrated that $\text{Ru}_3(\text{CO})_{12}$ catalyses tetramethyldisilazane and NH_3 dehydrocoupling to generate a mixture of cyclic, linear and branched silazane oligomers with turnover frequencies (TOFs) of up to 3438 h^{-1} relative to Si–H utilization at 90 °C.¹¹ In subsequent studies, this catalyst was used to dehydrocouple NH_3 with Et_2SiH_2 ,¹² HexSiH_3 ,¹³ PhSiH_3 ,¹³ and H-functionalized siloxanes.¹⁴ In 1991, Eisenberg obtained oligomers upon coupling NH_3 with Me_2SiH_2 using $\text{Rh}_2\text{H}_2(\text{CO})_2(\text{dppe})_2$,¹⁵ and the Corriu Group coupled NH_3 with MePhSiH_2 in the presence of $[\text{N}^n\text{Bu}_4][\text{F}]$ to yield oligocyclosilazanes.¹⁶ The following year, Liu and Harrod used Cp_2TiMe_2 to dehydrocouple NH_3 to Ph_2MeSiH , PhMeSiH_2 , and PhSiH_3 .¹⁷ Additionally, NH_3 has been coupled to 1,4-bis(dimethylsilyl)benzene to yield a polycarbosilazane¹⁸ and borylated secondary silanes to generate preceramic polymers.¹⁹

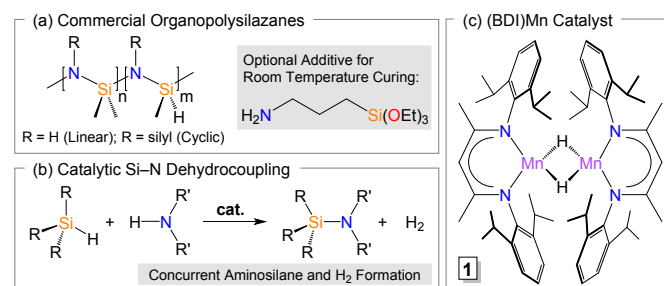


Fig. 1. (a) Organopolysilazanes, (b) Si–N dehydrocoupling, and (c) manganese catalyst **1**.

Upon preparing²⁰ and evaluating the electronic structure²¹ of the β -diketiminate (BDI) manganese hydride dimer, $[(2,6\text{-iPr}_2\text{PhBDI})\text{Mn}(\mu\text{-H})_2]$ (**1**, Fig. 1, c), our laboratory demonstrated that this compound mediates the dehydrocoupling of NH_3 and SiH_4 at 25 °C to prepare perhydropolysilazane, a ceramic precursor commonly used in microelectronics manufacturing.²² The use of **1** to dehydrocouple PhSiH_3 and OctSiH_3 with diamines allowed for the deposition of coatings from silane diamine

School of Molecular Sciences, Arizona State University, Tempe, AZ 85287, USA.
E-mail: ryan.trovitch@asu.edu

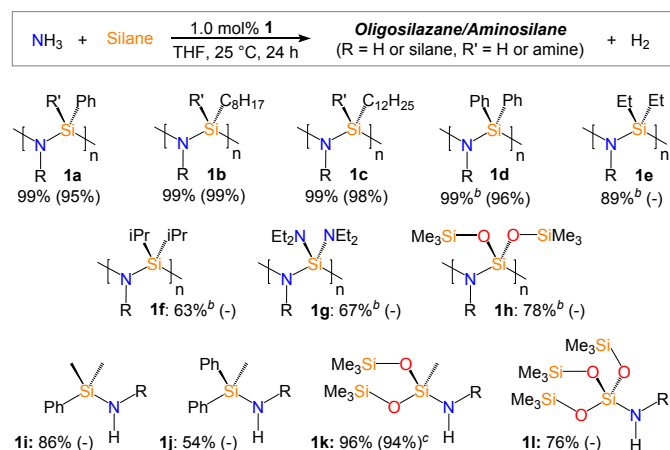
† Electronic supplementary information (ESI) available: General considerations, detailed procedures, and characterization data. See DOI: 10.1039/x0xx00000x

polymer solutions; however, drawbacks including a short shelf-life, cracking, and undesired tackiness were noted.²³ To address these shortcomings, this contribution expands the scope of Si–H sources that can be dehydrocoupled to NH₃ using **1**. Rather than focus on the ceramic applications targeted by Laine^{11–14} and Harrod,¹⁷ we demonstrate that Si–N dehydrocoupling can be used in place of ammonolysis to prepare an oligosilazane that affords corrosion-resistant coatings at room temperature.

Results and discussion

Starting with the optimized conditions of **1**-catalyzed Si–N dehydrocoupling,²³ this study began with the addition of 1 atm NH₃ to a thick-walled glass bomb containing PhSiH₃ and 1 mol% **1** dissolved in 5 mL THF. Intermittent freeze-pump-thaw cycles allowed for the removal of H₂ gas, and excess NH₃ was removed under dynamic vacuum after 24 h at 25 °C. After work up of the reaction in an inert atmosphere glovebox to prevent oxidation, ¹H NMR analysis revealed complete PhSiH₃ consumption (99% conv.) and a viscous oil identified as **1a** was isolated in 95% yield (Table 1). Similar conversions and yields were noted for the **1**-mediated coupling of NH₃ with octylsilane (**1b**) and dodecylsilane (**1c**); however, the latter afforded a waxy solid rather than an oil. Products **1a–1c** are believed to feature –NH₂ chain ends along with limited tertiary silicon (R' = hydrogen) and tertiary amine environments (R = silane) as judged by ¹H NMR and IR spectroscopic analysis, consistent with the use of excess NH₃.

Table 1. Dehydrocoupling of NH₃ with primary, secondary, and tertiary silanes using **1**.^a



^aPercent conversion relative to silane substrate, with isolated yields in parentheses. ^bPercent Si–H utilization. ^cObtained as a 12:1 ratio of disilylamine to silylamine.

The **1**-mediated formation of polysilazanes from secondary silanes was then explored. The dehydrocoupling of NH₃ and Ph₂SiH₂ allowed for complete Si–H utilization and the isolation of **1d** as a viscous oil in 96% yield. However, the use of Et₂SiH₂ (**1e**), iPr₂SiH₂ (**1f**), (Et₂N)₂SiH₂ (**1g**), or (Me₃SiO)₂SiH₂ (**1h**) did not allow for polysilazane isolation; the observation of unreacted and partially-coupled silanes with Si–H utilization values ranging from 63–89% is consistent with short-chain oligomer formation

(n = 3–7). Although the coupling of tertiary silanes with NH₃ is not capable of generating polysilazanes, **1** was used to aminate these reagents to identify substitution patterns that allow for siloxane crosslinking. Although complete conversion was not observed during the formation of **1i–1l**, the isolation of **1k** in 94% yield (96% conv.) offered an indication that hydrosiloxanes could be used for **1**-catalyzed dehydrocoupling.^{14,24,25}

Due to their moisture sensitivity, the molecular weight distributions of **1a–1h** could not be analyzed by gel permeation chromatography.²⁵ However, their full solubility in benzene-*d*₆ allowed for weight-average molecular weight (M_w) estimation via diffusion-ordered NMR spectroscopy (DOSY). The diffusion coefficients for **1a–1h** were obtained by following ¹H NMR signal attenuation as a function of pulsed field gradient strength and the corresponding values are provided in Table 2. These values were converted into hydrodynamic radii via the Stokes-Einstein equation and the M_w estimation method described by Grubbs²⁶ was applied. In general, the molecular weights of **1a–1h** were found to be quite modest. For example, **1a** was estimated to have a M_w of 2300 g/mol, which implies that the average chain features only 19 silazane units (the repeating units range from 119.20 g/mol if R and R' are substituents to 121.11 g/mol if R and R' = H). Lower M_w values of 450–600 g/mol were noted for **1e–1g**, further confirming short-chain oligomer formation. Therefore, **1a–1h** are best described as oligomers rather than polymers.

Table 2. Analysis of **1a–1h** by DOSY.

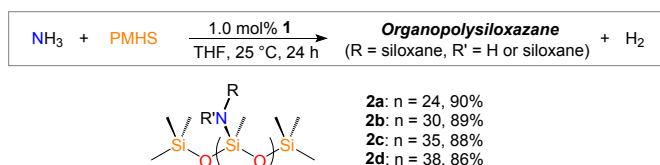
Product	Diffusion coefficient (10 ⁻¹⁰ m ² /s)	Hydrodynamic Radius (Å)	M _w (g/mol) ^a
1a	3.208	11.29	2300
1b	4.519	8.01	1200
1c	5.273	6.87	900
1d	6.119	5.92	700
1e	6.749	5.37	600
1f	7.37	4.91	500
1g	7.5	4.83	450
1h	3.79	9.56	1700
3g	2.27	15.95	4300

^aMolecular weight estimated in benzene-*d*₆ at 25 °C using the standard calibration curve reported by Grubbs.²⁶

Next, the coupling of NH₃ with polymethylhydrosiloxane (PMHS) was pursued in an effort to obtain polysiloxazane surrogates that more closely resemble commercial coatings than **1a–1d**. Adding 1 atm of NH₃ to a THF solution with 1 mol% **1** and PMHS featuring an average of 24 methylhydrosiloxane units per chain afforded **2a** as a white solid after 24 h at ambient temperature (Table 3). Likewise, repeating this experiment with siloxanes possessing an average of 30 (**2b**), 35 (**2c**), and 38 (**2d**) hydrides per chain yielded the corresponding polysiloxazanes in good yield. Although each solid was found to possess unreacted Si–H functionalities by IR spectroscopy, simultaneous thermal analysis suggested the presence of considerable crosslinking. For example, thermogravimetric analysis (TGA) of **2a** under N₂ revealed that only 5% of its original mass was lost upon heating to 735 °C and 91% was retained upon heating to 1,000 °C

(ceramic yield). Repeating the analysis under O₂ resulted in more significant weight loss of 6%, with an inflection point at 498 °C and a correlated differential scanning calorimetry (DSC) melt feature. Similar thermal properties were observed for **2b-2d**. While these characteristics may be of interest for the formation of high-temperature ceramics,^{11-14,17,25} the isolation of **2a-2d** as insoluble solids is not useful for coating applications.

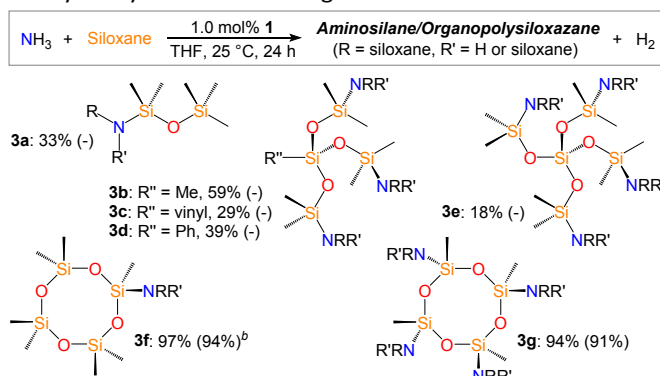
Table 3. Dehydrocoupling of NH₃ with PMHS using **1**.^a



^aIsolated yields are reported for each solid.

In addition to dehydrocoupling NH₃ with the linear siloxanes in Table 3, attempts were made to generate polysiloxazanes derived from branched and cyclic siloxane precursors. Adding 1 atm of NH₃ to the model substrate, pentamethyldisiloxane, in the presence of **1** allowed for only 33% Si–H utilization after 24 h (**3a**, Table 4). Unfortunately, this lack of conversion extended to the dehydrocoupling of tertiary (**3b-3d**) and quaternary (**3e**) siloxanes featuring terminal hydride functionalities. In contrast, 97% conversion was noted for heptamethylcyclotetrasiloxane (**3f**), and 94% Si–H utilization was observed for the perhydro-variant 1,3,5,7-tetramethylcyclotetrasiloxane (**3g**). Although **3g** was briefly isolated as an oil, it was found to solidify within 3 h at ambient temperature. Evaluation of this product by DOSY revealed a diffusion coefficient of 2.27 × 10⁻¹⁰ m²/s, a hydrodynamic radius of 15.95 Å, and an estimated M_w of 4300 g/mol.

Table 4. Dehydrocoupling of NH₃ with dimethylhydrosiloxanes and cyclic hydrosiloxanes using **1**.^a



^aPercent conversion of initial Si–H to Si–N with isolated yields in parentheses. ^bProduct obtained as a 9:1 ratio of disilylamine to silylamine.

After evaluating the scope of **1**-based ammonia and siloxane dehydrocoupling, **1a** was selected as a representative precursor for metal surface coating, in this case copper. Repeating the synthesis of **1a** in the absence of solvent resulted in the formation of a high viscosity silazane oil. This oil was sufficiently

thick to inhibit the dip-coating of copper tape; therefore, a 10% by weight solution in THF was prepared. Upon applying a single coat under N₂, the Cu surface was allowed to dry for 24 h and then cured in air for 24 h before being analyzed under a scanning electron microscope (SEM). At 1000× magnification, a few minor imperfections were observed (an arrow points to one in Fig. 2, a) across an otherwise uniform surface. Evaluating a cross-section of the tape (Fig. 2, b) revealed a thickness of 20 μm, which is more than sufficient for anti-corrosion applications (commercial formulations yield 10 μm coatings).²³ A single-coat thickness of this magnitude is not generally accessible from dilute polysilazane solutions.

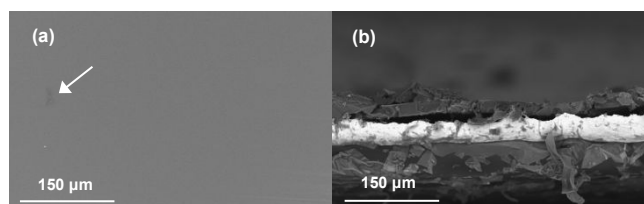


Fig. 2. (a) SEM image of Cu dip-coated with **1a** and (b) cross-section at 1000× magnification after 24 h of curing in air.

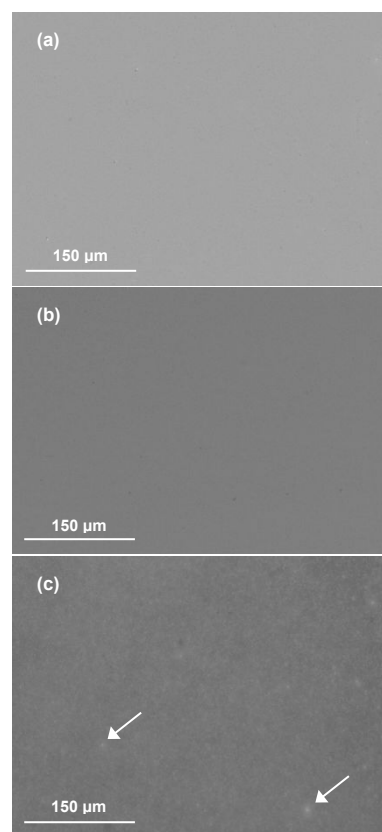


Fig. 3. (a) SEM image of Cu dip-coated with **1a** after curing in air for 24 h at 1000× magnification. (b) SEM image of cured coating after being submerged in H₂O for 24 h. (c) SEM image of cured coating after being submerged in 1.0 M HCl for 24 h.

To assess the corrosion resistance of **1a**-derived coatings, additional samples of Cu tape were dip-coated into a 10% by

weight solution of this oligomer in THF and allowed to cure in air at 25 °C for 24 h. Upon confirming the presence of a uniform surface at 1000× magnification (Fig. 3, a), one sample was submerged in deionized H₂O for 24 h while a second was placed in 1.0 M HCl. These samples were subsequently removed from solution and allowed to dry on a kimwipe for 24 h prior to SEM analysis. Notably, the coated Cu that had been placed in H₂O for 24 h was unmodified and no evidence for corrosion was noted by SEM (Fig. 3, b). The coating that was subjected to 1.0 M HCl for 24 h remained intact, but SEM analysis revealed roughening and obvious signs of pitting (Fig. 3, c, marked with arrows). It is important to note that 1.0 M HCl (pH = 0) is far more acidic than coatings would experience under environmental conditions (the transportation and construction industries rely on polysilazane coatings to protect steel and other metals from acid rain, which can have a pH as low as 4).

In prior work, the addition of **1** to solutions featuring an amine resulted in immediate hydrogen evolution and formation of the respective amido dimer.²² These intermediates, including crystallographically-characterised [(^{2,6}-iPr₂PhBDI)Mn(μ-NHiPr)]₂, were slightly darker in color than **1** but remained soluble, even in hydrocarbon solvents such as toluene. Throughout this study, each time NH₃ was added to a bomb containing a THF solution of **1** and organosilane, a yellow precipitate formed immediately upon warming the reaction to room temperature. To identify this precipitate, 0.2 g of **1** was dissolved in THF and NH₃ was added in the absence of silane, allowing for isolation of [(^{2,6}-iPr₂PhBDI)Mn(μ-NH₂)₂] (**2**, Fig. 4) as a yellow powder (90% yield).

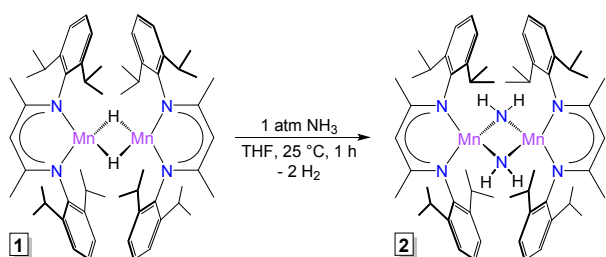


Fig. 4. Ammonia activation by **1** to form resting state **2**.

Recrystallisation of **2** from a low concentration THF solution at -35 °C afforded crystals suitable for X-ray diffraction. The solid-state structure of this compound was found to possess a pseudo-tetrahedral environment around each metal and a Mn(1)–Mn(1A) distance of 3.0423(12) Å (Fig. 5), comparable to the distance of 3.0487(6) Å observed for [(^{2,6}-iPr₂PhBDI)Mn(μ-NHiPr)]₂.²² Additional metrical parameters are provided in Table 5. Notably, the hydrogen atoms on the bridging NH₂ moieties of **2** were located in the difference map, confirming that these ligands are anionic and that the Mn centres are divalent. This compound was also found to exhibit a magnetic moment of 6.2 μ_B at 25 °C, which is consistent with weak coupling between two high-spin Mn(II) centres.²¹

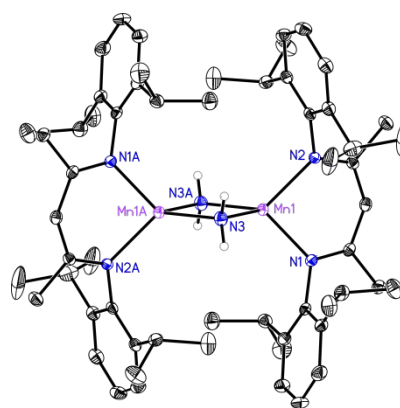


Fig. 5. Solid-state structure of **2**.

Table 5. Bond distances (Å) and angles (°) determined for **2**.

Bond Length (Å)		Angle (°)	
Mn1-N1	2.111(2)	N1-Mn1-N2	90.57(8)
Mn1-N2	2.117(2)	N1-Mn1-N3	121.48(9)
Mn1-N3	2.106(2)	N1-Mn1-N3A	117.56(8)
Mn1-N3A	2.122(2)	N2-Mn1-N3	122.50(8)
Mn1-Mn1A	3.0423(12)	N2-Mn1-N3A	119.96(8)

To confirm that **2** is a catalytically-relevant resting state (as opposed to a deactivation product), an isolated sample of this compound was added to excess PhSiH₃ in THF. To match the conditions of catalysis in Table 1, this solution was allowed to sit at room temperature for 24 h, after which time the solvent was removed and ¹H NMR spectroscopic analysis confirmed the formation of **1** (Fig. 6, a). To further demonstrate that **2** is relevant to the catalytic cycle, a THF solution featuring 1 mol% of isolated **2** relative to PhSiH₃ was placed in a thick-walled glass bomb and 1 atm of NH₃ was added. After 24 h at 25 °C, ¹H NMR spectroscopic analysis revealed >99% PhSiH₃ consumption and the formation of **1a** (obtained in 97% isolated yield, Fig. 6, b). This observation is noteworthy given that **2** has been found to catalyse the dehydrocoupling of NH₃ and PhSiH₃ with the same activity achieved for **1**.

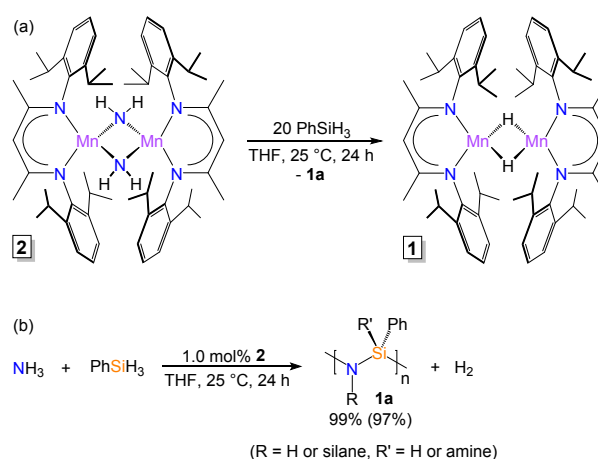


Fig. 6. (a) The conversion of resting state **2** to **1** in the presence of PhSiH₃. (b) The use of **2** as a catalyst for the dehydrocoupling of NH₃ and PhSiH₃.

These experiments are consistent with prior mechanistic analysis of **1**-catalysed Si–N dehydrocoupling.²² Following dissociation of **1** into monomeric hydrides (**Fig. 7**, with a barrier of 1.5 kcal/mol),²⁷ σ -bond metathesis between Mn–H and an incoming N–H bond of NH₃ results in the parent amido, (^{2,6}-iPr₂PhBDI)Mn(NH₂). Dimerization of this intermediate leads to the precipitation of **2** (often observed at the bottom of the flask). However, **2** is believed to reversibly dissociate into monomers that undergo σ -bond metathesis with an incoming Si–H bond to afford the Si–N product and regenerate (^{2,6}-iPr₂PhBDI)Mn(H).²² Since most of the Mn centers activate NH₃ and then precipitate to the bottom of the reaction, we believe that only a small percentage of the catalyst is active at any given time, leading to far lower TOFs (up to 4 h⁻¹ per substrate) than those observed for the **1**-mediated dehydrocoupling of silanes and diamines (300 s⁻¹).²⁴

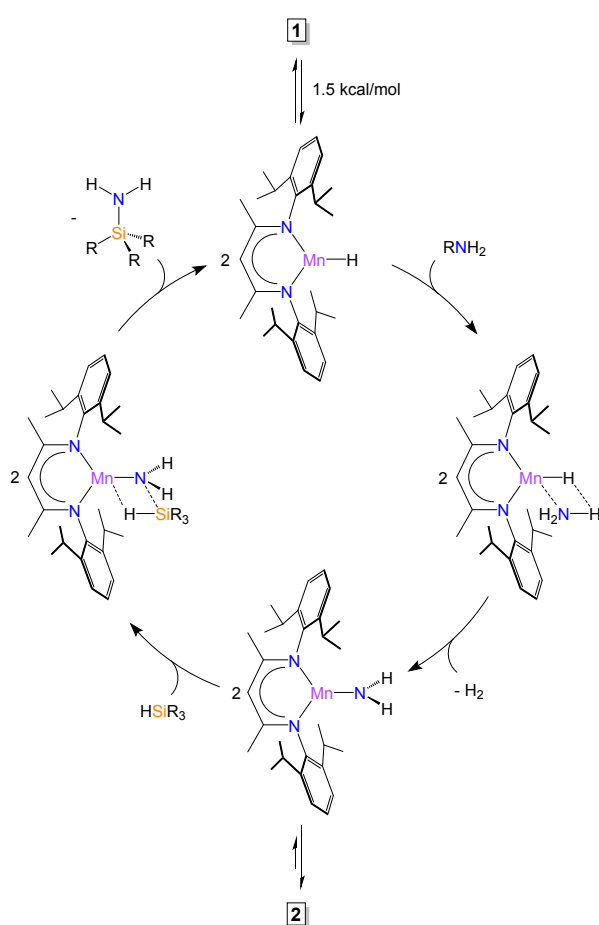


Fig. 7. Proposed NH₃ dehydrocoupling mechanism using **1** or **2**.

Conclusions

The ability of **1** to dehydrocouple NH₃ to silane and siloxane reagents at 25 °C has been described, representing the broadest Si–N dehydrocoupling scope for NH₃ explored to date. This methodology has proven to be effective for the preparation of oligosilazanes when using primary and secondary silanes and crosslinked polysiloxazane solids when using PMHS. Notably, a

representative oligosilazane product has been applied to a metal surface and cured to afford coatings that are comparable to commercial polysilazane coatings in appearance, thickness, and resistance to corrosion upon exposure to water. This contribution positions Si–N dehydrocoupling as a sustainable, halogen-free approach to preceramic coating synthesis.

Author contributions

G.K.M. is credited with investigation and formal analysis. T.T.N. is credited with investigation, formal analysis, and writing – original draft. M.F. is credited with investigation and formal analysis. R.J.T. is credited with conceptualization, funding acquisition, project administration, and writing – review & editing.

Conflicts of interest

Our laboratory retains rights to **1** and **2**, and their use for Si–N dehydrocoupling, through U.S. Patent 11,273,432 (2022).

Data availability

CCDC 2349466 contains the supplementary crystallographic data for this paper. This data can be obtained free of charge via www.ccdc.cam.ac.uk/data_request/cif. Additional data that support this article have been included as part of the Electronic Supplementary Information.

Acknowledgements

This material is based upon work supported by the National Science Foundation under Grant No. 2154359. We would like to acknowledge Dr. Thomas L. Groy for assistance with preparing X-ray crystallographic data. We thank the Long Group and Biodesign Center for Sustainable Macromolecular Materials and Manufacturing for SEM assistance.

Notes and references

- 1 E. G. Rochow, *Pure Appl. Chem.*, 1966, **13**, 247-262.
- 2 A. Lukacs, III and G. J. Knasiak, US Patent 6,652,978, 2003.
- 3 M. Weinmann, in *Silicon-based Inorganic Polymers*, ed. R. De Jaeger and M. Gleria, Nova Science Publishers, New York, 2008, ch. 7, pp. 371-414.
- 4 A. Margailan, C. Bressy and F.-X. Perrin, US Patent 9,676,946, 2017.
- 5 F. Bauer, U. Decker, A. Dierdorf, H. Ernst, R. Heller, H. Liebe and R. Mehnert, *Prog. Org. Coat.*, 2005, **53**, 183-190.
- 6 M. B. Reuter, K. Hageman and R. Waterman, *Chem. – Eur. J.*, 2021, **27**, 3251-3261.
- 7 V. Verma, A. Koperniku, P. M. Edwards and L. L. Schafer, *Chem. Commun.*, 2022, **58**, 9174-9189.
- 8 B. E. Leland, J. Mondal and R. J. Trovitch, *Chem. Commun.*, 2023, **59**, 3665-3684.
- 9 T. Mitsudome, T. Urayama, Z. Maeno, T. Mizugaki, K. Jitsukawa and K. Kaneda, *Chem. Eur. J.*, 2015, **21**, 3202-3205.
- 10 J. F. Dunne, S. R. Neal, J. Engelkemier, A. Ellern and A. D. Sadow, *J. Am. Chem. Soc.*, 2011, **133**, 16782-16785.

PAPER

Dalton Transactions

- 11 Y. Blum and R. M. Laine, *Organometallics*, 1986, **5**, 2081-2086.
- 12 Y. D. Blum, R. M. Laine, K. B. Schwartz, D. J. Rowcliffe, R. C. Bening and D. B. Cotts, *Mat. Res. Soc. Symp. Proc.*, 1986, **73**, 389-394.
- 13 K. A. Youngdahl, R. M. Laine, R. A. Kennish, T. R. Cronin and G. G. A. Balavoine, *Mat. Res. Soc. Symp. Proc.*, 1988, **121**, 489-496.
- 14 R. M. Laine, Y. D. Blum, R. D. Hamlin and A. Chow, in *Ultrastructure Processing of Ceramics, Glasses and Composites II*, ed. D. J. Mackenzie and D. R. Ulrich, John Wiley & Sons, New York, 1988, pp. 761-769.
- 15 W. D. Wang and R. Eisenberg, *Organometallics*, 1991, **10**, 2222-2227.
- 16 R. J. P. Corriu, D. Leclercq, P. H. Mutin, J. M. Planeix and A. Vioux, *J. Organomet. Chem.*, 1991, **406**, C1-C4.
- 17 H. Q. Liu and J. F. Harrod, *Organometallics*, 1992, **11**, 822-827.
- 18 Y. Li and Y. Kawakami, *Macromolecules*, 1999, **32**, 8768-8773.
- 19 M. Weinmann, S. Nast, F. Berger, G. Kaiser, K. Müller and F. Aldinger, *Appl. Organomet. Chem.*, 2001, **15**, 867-878.
- 20 T. K. Mukhopadhyay, M. Flores, T. L. Groy and R. J. Trovitch, *Chem. Sci.*, 2018, **9**, 7673-7680.
- 21 C. Oh, J. Siewe, T. T. Nguyen, A. Kawamura, M. Flores, T. L. Groy, J. S. Anderson, R. J. Trovitch and M.-H. Baik, *Dalton Trans.*, 2020, **49**, 14463-14474.
- 22 T. T. Nguyen, T. K. Mukhopadhyay, S. N. MacMillan, M. T. Janicke and R. J. Trovitch, *ACS Sustainable Chem. Eng.*, 2022, **10**, 4218-4226.
- 23 T. T. Nguyen, A. Sharma, T. L. P. Nguyen, M. A. Trimble, D.-K. Seo and R. J. Trovitch, *Green Chem.*, 2024, **26**, 5284-5292.
- 24 Z. Lu, K. Murakami, S. Koge, T. Mizumo and J. Ohshita, *J. Organomet. Chem.*, 2016, **808**, 63-67.
- 25 A. Sharma, R. H. Bean, T. E. Long and R. J. Trovitch, *ACS Sustainable Chem. Eng.*, 2023, **11**, 11172-11180.
- 26 W. Li, H. Chung, C. Daeffler, A. J. Johnson and R. H. Grubbs, *Macromolecules*, 2012, **45**, 9595-9603.
- 27 T. T. Nguyen, J.-H. Kim, S. Kim, C. Oh, M. Flores, T. L. Groy, M.-H. Baik and R. J. Trovitch, *Chem. Commun.*, 2020, **56**, 3959-3962.

Data Availability Statement

CCDC 2349466 contains the supplementary crystallographic data for this paper. This data can be obtained free of charge via www.ccdc.cam.ac.uk/data_request/cif. Additional data that support this article have been included as part of the Electronic Supplementary Information.